

Search for dark matter production in association with the Z' boson at the LHC in pp collisions at $\sqrt{s} = 8$ TeV using Monte Carlo simulations

S. Elgammal* and M. A. Louka†

Centre for theoretical physics, The British University in Egypt, Cairo

A. Y. Ellithi and M. T. Hussein

Physics Department, Faculty of Science, Cairo University.

(Dated: May 28, 2021)

This analysis presents the possibility for the search for Dark Matter (DM) particles using events with a Z' heavy gauge boson and a large missing transverse momentum at the Large Hadron Collider (LHC). We consider the muonic decay of Z' . The analyzed Monte Carlo samples were the Open simulated files produced by the CMS collaboration for proton-proton collisions correspond to an integrated luminosity of the LHC run-I with 19.7 fb^{-1} at $\sqrt{s} = 8$ TeV. Two scenarios, one simplified benchmark scenario so called Dark Higgs and the effective field theory (EFT) formalism, were used for interpretations. Limits are set on both Z' , dark matter masses and the cutoff scale of the EFT.

Keywords: Dark matter, New heavy gauge boson, The Large Hadron Collider LHC, The Compact Muon Solenoid CMS

I. INTRODUCTION

One of the interesting open questions in modern physics, that can be explored within the current research, is the existence of a new type of non-luminous matter, which can be possibly made up of non-baryonic particles called Dark Matter (DM). The need of a DM hypothesis arises from several astrophysical observations and it is supposed that DM contributes to about 27% of the mass of the Universe [1–9]. In parallel to the evidence from astrophysical constrains, direct search for DM at the Large Hadron Collider (LHC) is ongoing using proton-proton collision events with a signature based on large missing transverse momentum. The methodology of the direct detection of DM at the particle colliders is implemented in the "Mono-X" models, which predict the production of a visible state particle plus missing transverse momentum recoiling against that particle, and is interpreted as the production of dark sector particles with the signature $X + \cancel{p}_T$. The visible particle could be a standard model (SM) particle, i.e. W, Z or jets [10], photon [11] or Higgs [12]. DM particles have also been searched for in events with dilepton from Z boson decay plus large missing transverse momentum with centre-of-mass energies $\sqrt{s} = 8$ [13] and 13 TeV [14].

The same idea has been extended to beyond the standard model (BSM) particles [15, 16]. The model we study (Mono- Z') predicts the production of DM in association with the new heavy gauge boson denoted by Z' . These dark sector particles can be identified in the detectors located at the LHC as a large missing energy [17]. The Z' boson is considered as a new particle in many of BSM theories and some extensions of the SM, e.g. the

grand unification scenarios. The Z' is neutral, and has the same decay modes of the standard model Z boson with a larger spectra of masses. More information can be found in [18–21]. Hence, the search for new heavy resonance in the hadronic and leptonic channels is one of the important goals of high energy physics, in order to investigate those BSM hypotheses that predict new sort of bosons. The ATLAS collaboration in [22] studied the previously mentioned Mono- Z' model considering the hadronic decay of Z' boson. The coupling of Z' to electrons is constrained previously by LEP measurements in [23], thus in our analysis we consider the muonic decay of Z' (i.e. $Z' \rightarrow \mu^+ \mu^-$).

Thanks to the CMS open data project [24], since the CMS collaboration have published significant amounts of recorded and simulated pp collision data at $\sqrt{s} = 8$ TeV, which are available for all scientists even if they are not members of the CMS collaboration. In our study we use only the CMS simulated samples. These samples have a great potential and offer opportunities to evaluate the cross sections of the SM processes, to model the SM backgrounds for different studies and to perform further analysis, as reported in [25].

In this paper we first give a more detailed description of the theoretical model which predicts the possible production of DM in association with the heavy gauge boson (Z') in section II, while in section III we briefly describe the Compact Muon Solenoid (CMS) detector. In section IV we discuss the simulated samples, for signals and SM background sources, used in the analysis. That is followed in section V by the discussion of the backgrounds in this search and the methods with which their contributions are estimated. The selection of events and the general strategy of the search are outlined in section VI. Systematic uncertainties affecting on the prediction of backgrounds are presented in section VII. The results and summary of the search are respectively

* sherif.elgammal@bue.edu.eg

† Also at Cairo University

addressed in section VIII and section IX.

II. MONO-Z' MODEL

The work done in [17] proposed the production of dark matter with a resonance which comes from heavy Z' gauge boson, this model is known as the Mono- Z' model. The model has been presented in three different possible scenarios which are two simplified models, the dark Higgs (DH) and the light vector (LV) or also called the dark fermion, in addition to a third scenario which is known as light vector with inelastic effective field theory coupling (EFT). The two simplified models are represented in figure 1. In the DH scenario, the mediator vector boson Z' is produced via $q\bar{q}$ annihilation process, at parton level, then it undergoes a dark-higgs-strahlung process analogous to the emission of the SM higgs particle by the W or Z bosons. The new scalar coupled to the Z' is called the dark higgs (h_D), and it is assumed that the dark higgs decays rapidly into a pair of dark sector particles ($\chi\bar{\chi}$). The coupling of Z' with h_D is given by $(g_{DM}M_{Z'}h_D Z'_\mu Z'^\mu)$ and the coupling of it with quarks is $(g_{SM}\bar{q}\gamma^\mu q Z'^\mu)$. The Feynman diagram of the process is shown in figure 1(a).

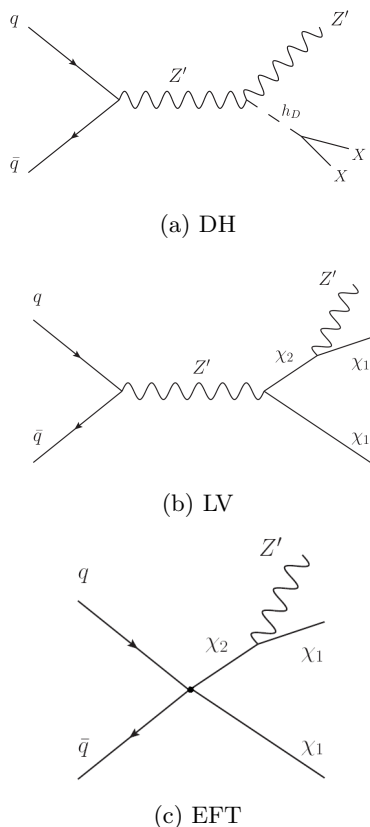


Figure 1 Feynman diagrams for the mono- Z' simplified scenarios; dark higgs (a) and light vector (b), and the EFT scenario (c) [17].

Scenario	Masses assumptions
Light dark sector	$M_{h_D} = \begin{cases} M_{Z'}, & M_{Z'} < 125 \text{ GeV} \\ 125 \text{ GeV}, & M_{Z'} > 125 \text{ GeV} \end{cases}$
Heavy dark sector	$M_{h_D} = \begin{cases} 125 \text{ GeV}, & M_{Z'} < 125 \text{ GeV} \\ M_{Z'}, & M_{h_D} > 125 \text{ GeV}. \end{cases}$

Table I The mass assumptions chosen in the light and heavy dark sector cases for the dark higgs scenario [17].

There are two assumptions for setting masses in the DH scenario, which are illustrated for the light dark sector and the heavy dark sector in table I.

For the light vector scenario; one of the dark particles is sufficiently heavier than Z' , so that it can decay to Z' plus another light dark particle ($\chi_2 \rightarrow Z'\chi_1$) as shown in figure 1(b). The interaction term, in Lagrangian, between the dark particles and Z' is given by

$$\frac{g_{DM}}{2} Z'_\mu (\bar{\chi}_2 \gamma^\mu \gamma^5 \chi_1 + \bar{\chi}_1 \gamma^\mu \gamma^5 \chi_2),$$

where χ_1 is a final state dark sector stable particle. For the mass assumptions in case of the LV scenario; the heavy dark particle (χ_2) should have a mass twice the mass of Z' , while the mass of light dark particle (χ_1) is half of the mass of Z' .

In the rest of this paper, the coupling of Z' with the SM fermions (quarks and leptons) will be referred to as g_{SM} , and the coupling with the DM particles will be denoted by g_{DM} . The total decay widths of Z' and h_D (Z' and χ_2) in the DH (LV) cases, are calculated regarding the mass values of Z' and the coupling constants, assuming that Z' boson can only decay into a pair of muons and radiate an h_D boson in the DH scenario, and assuming that the decays $Z' \rightarrow \chi_1 \chi_2$, $\chi_2 \rightarrow Z' \chi_1$ and $Z' \rightarrow \mu \bar{\mu}$ are the only allowed for the LV scenario.

In these scenarios there are many free parameters, including the mediator mass $M_{Z'}$, the mass of the heavy dark particle M_{χ_2} , the mass of the light dark particle M_{χ_1} and the coupling constants (g_{SM} and g_{DM}). In this analysis, the values of the couplings ($g_{SM} = 0.25$ and $g_{DM} = 1.0$) have been chosen based on the results presented in [17] and [22]. The cross section measurements times branching ratios for the two simplified models (DH and LV) at different masses of Z' are compared in table II, and are calculated with Madgraph [26] at next-to-leading order (NLO).

Finally, the EFT scenario reduces the interactions between the DM particles and the SM fields down to contact interaction as given in the following interaction term

$$\frac{1}{2\Lambda^2} \bar{q} \gamma^\mu q (\bar{\chi}_2 \gamma^\mu \gamma^5 \chi_1 + \bar{\chi}_1 \gamma^\mu \gamma^5 \chi_2)$$

The Feynman diagram, which illustrates this process, is shown in figure 1(c). The assumptions for the masses

are the same set of the LV scenario. The production cross section measurements times branching ratios as a function of the scenario cutoff scale (Λ) are given in table III.

$M_{Z'}$ (GeV/c ²)	$\sigma \times \text{BR}$ (pb) Dark Higgs	$\sigma \times \text{BR}$ (pb) Light Vector
150	7.086×10^{-2}	1.734×10^{-2}
200	2.366×10^{-2}	0.507×10^{-2}
250	9.555×10^{-3}	1.808×10^{-3}
300	4.368×10^{-3}	0.738×10^{-3}
350	2.100×10^{-3}	0.318×10^{-3}
400	1.040×10^{-3}	0.140×10^{-3}
450	0.569×10^{-3}	0.069×10^{-3}
500	3.283×10^{-4}	0.355×10^{-4}
600	1.191×10^{-4}	0.104×10^{-4}
700	4.725×10^{-5}	0.333×10^{-5}

Table II The cross section measurements times branching ratios calculated at different masses of the Z' boson with the heavy dark sector assumption for the two simplified models (DH and LV), with the coupling constants $g_{SM} = 0.25$, $g_{DM} = 1.0$, at $\sqrt{s} = 8$ TeV.

$\Lambda(\text{TeV})$	$\sigma \times \text{BR}$ (pb)
1.0	0.0704
1.5	0.0139
2.0	0.0044
2.5	0.0018
3.0	0.00087
3.5	0.00047
4.0	0.000275

Table III The EFT production cross section measurements times branching ratios as a function of the scenario cutoff scale of the EFT(Λ), for a fixed mass point of Z' ($M_{Z'} = 450$ GeV) and centre-of-mass energy $\sqrt{s} = 8$ TeV.

The typical signature of these processes consists of a pair of opposite sign leptons or hadronic jets from the decay of Z' plus a large missing transverse momentum due to the stable dark sector particles χ and χ_1 . These two scenarios were previously studied by the ATLAS collaboration in [22] with the hadronic decay of Z' . In our study, we have considered the heavy dark sector assumption mentioned in table I, at which the signal region is shifted away from the background region due to a larger missing energy that assumed in this option, i.e the signal is more distinguishable from the background for the heavy dark sector assumption rather than the light one. The muonic decay of the on-shell Z' is considered since the CMS detector has been optimized to this decay channel. So that our the events are with the following topology $\mu^+ \mu^- + \cancel{E}_T$.

We studied one of these two simplified models which is the DH scenario, since it has a higher cross section than the LV, in addition to the EFT scenario. The behavior of

the cross sections times branching ratios with the mass of Z' , at $\sqrt{s} = 8$ and 13 TeV for the DH scenario, is shown in figure 2. As expected, the cross section measurements times branching ratios drop with the increase of the Z' mass. Moreover, we observe the increase in the cross section at higher \sqrt{s} (13 TeV), which is an advantage of the LHC run-II data with respect to run-I, as well as the ratio between the cross sections in the two cases increases with the mass of Z' , and reaches its maximum value (around 5 times) for the scanned range at $M_{Z'} = 700$ GeV, which indicates that the cross section drops slower in the case of $\sqrt{s} = 13$ TeV.

Table IV indicates the cross section measurements times branching ratios calculated for different sets of the Z' and χ masses. The cross section is not sensitive to the change in the dark matter particle mass, for this reason we work on the diagonal points for our purpose to put a limit on this parameter which will be discussed in the results.

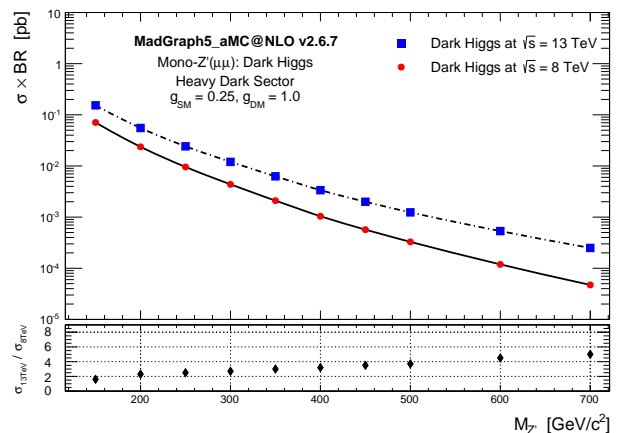


Figure 2 The behavior of the cross section measurements times branching ratios with the mass of Z' boson for the Dark Higgs scenario at $\sqrt{s} = 8$ TeV represented by red dots and 13 TeV represented by blue square. The lower panel indicates to the ratio of the cross sections between the two cases.

III. THE CMS DETECTOR

The Compact Muon Solenoid (CMS) detector (described in details at references [27, 28]) is one of the four main apparatus that have been built on the LHC at CERN. The 3-m-long and 5.9-m-inner diameter superconducting solenoid provides a 3.8-T magnetic field that delivers the bending power required to measure the momenta of the high energy charged particles. The solenoid accommodates the tracking system (pixel detector and silicon tracker) and the two calorimeters: the Electromagnetic Calorimeter (ECAL) has been designed to detect and measure electrons and photons and the Hadronic Calorimeter (HCAL) used to detect

$M_{Z'}/(\text{GeV})$	150	200	300	325	350	375	400	425	450	475	500
1	7.10×10^{-02}	2.36×10^{-02}	0.438×10^{-02}	0.305×10^{-02}	0.2107×10^{-02}	0.144×10^{-02}	0.1036×10^{-02}	0.764×10^{-03}	0.568×10^{-03}	0.428×10^{-03}	0.328×10^{-03}
5	7.08×10^{-02}	2.37×10^{-02}	0.437×10^{-02}	0.306×10^{-02}	0.210×10^{-02}	0.144×10^{-02}	0.104×10^{-02}	0.763×10^{-03}	0.569×10^{-03}	0.427×10^{-03}	0.3283×10^{-03}
10	7.10×10^{-02}	2.36×10^{-02}	0.037×10^{-02}	0.305×10^{-02}	0.211×10^{-02}	0.145×10^{-02}	0.104×10^{-02}	0.763×10^{-03}	0.569×10^{-03}	0.429×10^{-03}	0.328×10^{-03}
25	7.10×10^{-02}	2.358×10^{-02}	0.437×10^{-02}	0.305×10^{-02}	0.211×10^{-02}	0.144×10^{-02}	0.1035×10^{-02}	0.763×10^{-03}	0.568×10^{-03}	0.429×10^{-03}	0.329×10^{-03}
50	7.13×10^{-02}	2.36×10^{-02}	0.437×10^{-02}	0.306×10^{-02}	0.210×10^{-02}	0.144×10^{-02}	0.1038×10^{-02}	0.756×10^{-03}	0.567×10^{-03}	0.429×10^{-03}	0.328×10^{-03}
75	16.40×10^{-02}	2.36×10^{-02}	0.436×10^{-02}	0.305×10^{-02}	0.209×10^{-02}	0.144×10^{-02}	0.104×10^{-02}	0.763×10^{-03}	0.568×10^{-03}	0.429×10^{-03}	0.328×10^{-03}
100	8.98×10^{-07}	5.43×10^{-02}	0.436×10^{-02}	0.3052×10^{-02}	0.211×10^{-02}	0.144×10^{-02}	0.1039×10^{-02}	0.764×10^{-03}	0.568×10^{-03}	0.428×10^{-03}	0.326×10^{-03}
125	1.54×10^{-07}	5.01×10^{-07}	0.437×10^{-02}	0.3049×10^{-02}	0.209×10^{-02}	0.144×10^{-02}	0.104×10^{-02}	0.758×10^{-03}	0.567×10^{-03}	0.429×10^{-03}	0.327×10^{-03}
150	4.09×10^{-08}	1.0×10^{-07}	1.00×10^{-02}	0.3047×10^{-02}	0.2094×10^{-02}	0.144×10^{-02}	0.1037×10^{-02}	0.758×10^{-03}	0.567×10^{-03}	0.427×10^{-03}	0.326×10^{-03}
175	1.3×10^{-08}	3.05×10^{-08}	1.753×10^{-07}	3.766×10^{-07}	0.48×10^{-02}	0.1436×10^{-02}	0.1035×10^{-02}	0.756×10^{-03}	0.556×10^{-03}	0.427×10^{-03}	0.326×10^{-03}
200	5.25×10^{-09}	1.0×10^{-08}	4.36×10^{-08}	6.56×10^{-08}	1.04×10^{-07}	2.08×10^{-07}	0.239×10^{-02}	0.76×10^{-03}	0.566×10^{-03}	0.427×10^{-03}	0.325×10^{-03}

Table IV The Dark Higgs cross section measurements times branching ratios (pb) calculated for different sets of the masses M_χ and $M_{Z'}$ in GeV, for the heavy dark sector mass assumption, with the following couplings constants $g_{SM} = 0.25$, $g_{DM} = 1.0$ and $\sqrt{s} = 8$ TeV.

and measure the hadronic particles. The muon system envelope the above layers, the muon stations consist of many Drift Tubes (DT) layers in the barrel part and Cathode Strip Chambers (CSC) in the endcap region. The two parts are completed by the Resistive Plate Chambers (RPC).

The interaction point is considered to be the origin of the CMS coordinate system. The x-axis points toward the center of the LHC, the y-axis points upward and the z-axis is alongside the beam axis. The polar angle θ is measured from the positive direction of the x-axis, and the azimuthal angle ϕ is measured from the x-y transverse plan. However, the directions of the particles yield from the collision spot mostly expresses in terms of the pseudorapidity which defined as $\eta = -\ln[\tan(\theta/2)]$. For our purpose, we mention the reconstruction of muons and the missing transverse momentum. The muon object is identified and reconstructed from a global fit between the muon system and the inner tracker hence, it is referred to as global muons [29, 30]. The missing transverse momentum reconstruction is based on the Particle Flow algorithm described in references [28, 31], it is reconstructed as an imbalance in the vector sum of momenta in the transverse plan. i.e. it could be defined as the negative vector sum of the momenta of all particle flow reconstructed objects as $\vec{p}_T = -\sum \vec{p}_T^{pf}$ [32]. The magnitude of \vec{p}_T can be affected by many factors which cause underestimate or overestimate of its true value. These factors are basically related to the calorimeters response, and inefficiencies in the tracker, and non-linearity of the response of the calorimeter for hadronic particles. This bias can be effectively reduced by correcting for the p_T of the jets using jet energy corrections as defined in the following formula, which is given in [32]

$$\vec{p}_T^{\text{corr}} = \vec{p}_T - \sum_{jets} (\vec{p}_{Tjet}^{\text{corr}} - \vec{p}_{Tjet}),$$

where "corr" refers to the corrected values. Thus variables of particular relevance to the present analysis are the corrected missing transverse momentum vector \vec{p}_T^{corr} and the magnitude of this quantity, p_T^{corr} .

IV. SIMULATED SAMPLES

A. Monte Carlo simulation of the model signals

The model signal events are generated using MadGraph5_aMC@NLO v2.6.7 [26] which is a general purpose matrix element event generator. The cross section calculated at next to-leading-order (NLO) and the hadronization process has been done with Pythia [33]. The detector simulation, simulation of read out system response (digitization) and reconstruction processes have been done using the standard CMS open data software framework (the release CMSSW_5.3.32) at $\sqrt{s} =$

8 TeV requirements, with the suitable triggers list used for CMS-2012 analysis. We scanned the DH production cross section at different sets of the masses of the particles Z' and χ as free parameters covering a wide range for the mass of Z' boson from 150 GeV to 550 GeV and from 1 GeV to 200 GeV for the mass of χ , and the production cross section of the EFT at the range of Λ from 1.0 to 4 TeV, assuming $g_{SM} = 0.25$ and $g_{DM} = 1.0$ for all simulations.

B. Monte Carlo simulation of the SM backgrounds

In order to simulate the SM processes that have muons and/or missing energy (due to the undetected neutrinos) at the final state which could interface with our signal events, we used the CMS open Monte Carlo samples at $\sqrt{s} = 8$ TeV as background processes [24]. The Drell-Yan (DY) background (the production of a virtual Z/γ^* that decay into a muon pair) which is the dominant background, has been generated using Powheg [34]. Another important sources of SM background with dimuons in the final state are the fully leptonic decay of $t\bar{t}$ which is generated using MadGraph [26], the production of electroweak diboson channels as WW, WZ have been generated with MadGraph, and $ZZ \rightarrow \mu^-\mu^+\mu^-\mu^+$ process which is also generated with Powheg. The generation process for the mentioned samples are interfaced with Pythia v6.4.26 [33] for the modeling of parton shower. The Monte Carlo samples used in this analysis and their corresponding cross sections, calculated at next-to-leading or next-to-next-to-leading order, are indicated in table V.

V. BACKGROUNDS ESTIMATION

There are three main types of SM background to new physics search in the dimuon channel. The most significant is the irreducible SM Drell-Yan process. New physics can interfere with this process, if not mitigated, the effects can be significant. The second most important background type comes from muons from non-singularly produced W and Z bosons. The dominant source of these muons are from $t\bar{t}$ events although WW events become increasingly important at high mass as the boost of the top quark means that the b-jet enters the muons isolation cone and so the muon fails isolation requirements. Other sources include WZ and ZZ events although they are small compared to $t\bar{t}$ and WW. This background is referred to as $t\bar{t}$ and $t\bar{t}$ -like background as it is dominated by $t\bar{t}$. The third background is the jets background, where one or more jets are misidentified and incorrectly reconstructed as a muon, mainly arising from W+jet and QCD multijet. The contamination of jets background is usually estimated from data using a so called data driven method which is explained in [36], which is irrelevant for our study, since our analysis based mainly on MC simulations. In this analysis; the DY background and other

backgrounds from muons arising from non-singularly produced W and Z bosons is estimated directly from Monte Carlo simulation as in the other 8 TeV similar analysis [36]. The leptonic decay of $t\bar{t}$, WW and WZ are generated using Madgraph, while ZZ is generated using POWHEG. The Monte Carlo samples and their cross sections are documented in tables V, and normalized to their respective NLO or NNLO cross sections. Another source of background to this analysis is the cosmic muons contribution, which is suppressed by constraining the vertex position as discussed in section VI A, and also by constraining the impact parameter of the muons relative to the vertex position as in the high P_T muon identification [43, 44], this contribution is also negligible.

VI. EVENTS SELECTION AND ANALYSIS STRATEGY

A. Preselection of events

The preselection criteria is based on the high p_T muon identification [43, 44], which was applied in the 2012 analysis for the search for heavy resonances in the dilepton channel [36]; in addition the off-line muon reconstructed transverse momentum (p_T^μ) is selected to be higher than 45 GeV in order to be fully efficient for the trigger used (HLT_Mu40_eta2p1), and the detector acceptance is restricted to the range $|\eta^\mu| < 2.1$ of the reconstructed pseudorapidity. The preselection criteria is indicated in table VI, at which muon candidates must be reconstructed as "global" muons, i.e. standalone muon object reconstructed in the muon system must match with an inner tracker's track to form the global muon object used later for our analysis. The muon candidates should be isolated; thus they have to pass a cut based on the relative tracker isolation, which is the scalar sum of the p_T of all other tracks within a cone of $\Delta R = \sqrt{(\Delta\eta)^2 + (\Delta\phi)^2} < 0.3$ around and not containing the muon's tracker track, this sum must be less than 10% of the muon's transverse momentum (p_T). Tracks used in the tracker isolation calculation have to originate within $\Delta Z = 0.2$ cm of the primary vertex, with which the muon candidate is associated [36].

The muon's transverse impact parameter with respect to the primary vertex, as measured by the tracker-only fit, must be smaller than 0.2 cm, which is a powerful cut to reject the cosmic muons that pass at the empty time between two bunch-crossing. Another cut is provided to reject cosmic muons that pass near the interaction point in-time with a bunch-crossing, is the 3D angle between the muon pairs, it is selected to be less than $\pi - 0.02$ rad [36]. Extra qualification cuts are applied such that, the muon pairs must be two opposite-sign and the χ^2/dof for the common vertex fitting is less than 10 [36], where χ is a state vector that describe the particle's track in each point of its trajectory, this method based on the minimization of χ^2/dof using the Kalman filter tech-

Process	Generator	Data Set Name	$\sigma \times \text{BR}$ (pb)	Order
$DY \rightarrow \mu\bar{\mu}$	Powheg	DYToMuMu_M-20_CT10_TuneZ2star_v2.8TeV. [38]	1916	NNLO
$t\bar{t} + \text{jets}$	Madgraph	TTJets_FullLeptMGDecays.8TeV. [39]	23.89	NLO
WW + jets	Madgraph	WWJetsTo2L2Nu_TuneZ2star.8TeV. [40]	5.8	NLO
WZ + jets	Madgraph	WZJetsTo3LNu.8TeV_TuneZ2Star. [41]	1.1	NNLO
$ZZ \rightarrow 4\mu$	Powheg	ZZTo4mu.8TeV. [42]	0.077	NLO

Table V CMS open MC samples used to simulate the SM background for pp collision at $\sqrt{s} = 8$ TeV, their corresponding cross section times branching ratio for each process and the order of calculations. The data set names and the used generators are stated.

nique, described in references [45, 46], is implemented in the CMSSW, this fitting is important in order to make correct pairing of muons that originate from the same vertex and for the rejection of the pile-up muons. Thus the events are selected with two opposite charge high p_T muons, with one of them passed the single muon trigger HLT_Mu40_eta2p1.

variable	cut value
High p_T muon ID	[43, 44]
p_T^μ (GeV)	> 45
$ \eta^\mu $ (rad)	< 2.1
$M_{\mu^+\mu^-}$ (GeV)	> 50

Table VI The preselection selection criteria based on single muon trigger requirement (HLT_Mu40_eta2p1), muon kinematic cuts and the high P_T muon ID.

Figure 3 illustrates the distribution of the dimuon invariant mass; the green histogram represents the Drell-Yan background, the blue histogram stands for the vector boson pair backgrounds (WW, WZ and ZZ) and the $t\bar{t} + \text{jets}$ background is represented by the grey histogram. These background histograms are stacked, while the signal models with different masses of the Z' heavy boson are represented by different colored lines, and are overlaid. The corresponding distribution of the missing transverse momentum is shown in figure 4. As the signal models are overwhelmed by the backgrounds, it is necessary to apply a more clever set of cuts to discriminate signals from SM backgrounds as will be explained in the next section. The number of dimuon events passing the preselection for each SM background processes and for the model signals are quoted in table VII for an integrated luminosity of 19.7 fb^{-1} . Uncertainties include both statistical and systematic components, summed in quadrature.

B. Events selection

After applying the preselection set of cuts, at which each event must have exactly two oppositely charged muons with $p_T^\mu > 45$ GeV, $|\eta^\mu| < 2.1$ each and one of these two muons should pass the single muon trigger (HLT_Mu40_eta2p1), the extra tighter selection has been optimized for DM signals in order to distinguish them

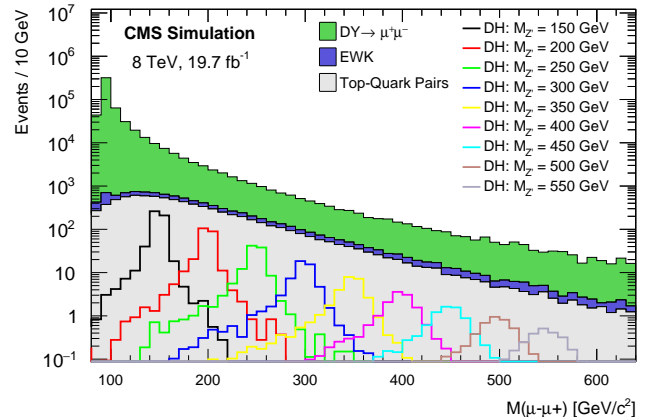


Figure 3 The measured dimuon invariant mass spectrum, after applying preselection cuts listed in table VI, together with the estimated SM backgrounds and Z' masses produced according to the dark Higgs model.

process	No. of events
$DY \rightarrow \mu^+\mu^-$	533515 ± 127708
$t\bar{t} + \text{jets}$	8363 ± 2004
WW + jets	1506 ± 362.7
WZ + jets	608 ± 147.8
$ZZ \rightarrow 4\mu$	58 ± 15.9
Sum Bkgs	544050 ± 130230
DH Signal (at $M_{Z'} = 450$ GeV)	8.2 ± 3.5
EFT Signal (at $\Lambda = 2$ TeV)	64.2 ± 17.3

Table VII The number of dimuon events passing the preselection for each SM background processes, the DH model and the EFT model; corresponding to an integrated luminosity of 19.7 fb^{-1} . Uncertainties include both statistical and systematic components, summed in quadrature.

from SM background and to obtain the best expected limit. The final selection is based on three variables: (1) The mass of the dilepton system ($M_{\mu^+\mu^-}$) is required to be within $(0.9 \times M_{Z'}) < M_{\mu^+\mu^-} < (M_{Z'} + 25)$ to be consistent with leptons from the heavy Z' boson decay,

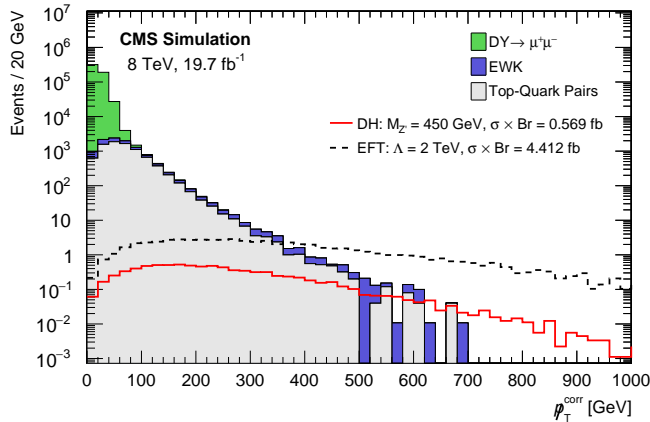


Figure 4 The missing transverse momentum distribution, after the preselection cuts listed in table VI; the colored stacked histograms refer to the MC simulation of the SM backgrounds, with two signals presentation of the model corresponding to the DH scenario with $M_{Z'} = 450$ GeV and to the EFT scenario with $\Lambda = 2$ TeV are superimposed. The signals are normalized to the product of cross section times the $Z' \rightarrow \mu^+\mu^-$ branching ratio.

(2) the azimuthal angle difference between the dimuon system and the missing transverse energy $\Delta\phi_{\mu^+\mu^-, \vec{p}_T^{\text{corr}}}$ and (3) the relative difference between the dimuon system transverse momentum and the missing transverse momentum $|p_T^{\mu^+\mu^-} - \vec{p}_T^{\text{corr}}|/p_T^{\mu^+\mu^-}$. Here $p_T^{\mu^+\mu^-}$ is the dimuon transverse momentum, and $\Delta\phi_{\mu^+\mu^-, \vec{p}_T^{\text{corr}}}$ is defined as difference in the azimuth angle between the dimuon system direction and the missing transverse momentum direction (i.e. $\Delta\phi_{\mu^+\mu^-, \vec{p}_T^{\text{corr}}} = |\phi^{\mu^+\mu^-} - \phi^{\text{miss}}|$) as indicated in table VIII.

1. Selection efficiency

The selection efficiency is defined as the ratio between the number of events after applying the cut-based final events selection summarised in table VIII and the number of events after the application of the preselection cuts, as defined in table VI. These efficiencies are calculated for both dark Higgs scenario (with $M_{Z'} = 450$ GeV) simulated sample and SM background sources, while error bars are statistical only. The selection efficiencies are listed in percentage in table IX, and also shown in figure 5. The cut-based final events selection criteria described above is designed to reduce the background events with the minimal possible effect on the signal events. After applying the full selection listed in table VIII, most of the backgrounds events are strongly suppressed to less than a percent for each of the SM backgrounds, while

we lose only around 34% of the dark Higgs signal events. Nevertheless in the signal region ($\vec{p}_T^{\text{corr}} > 200$ GeV) the efficiency of the DH signal is around 80%, which proves the success of this selection criteria.

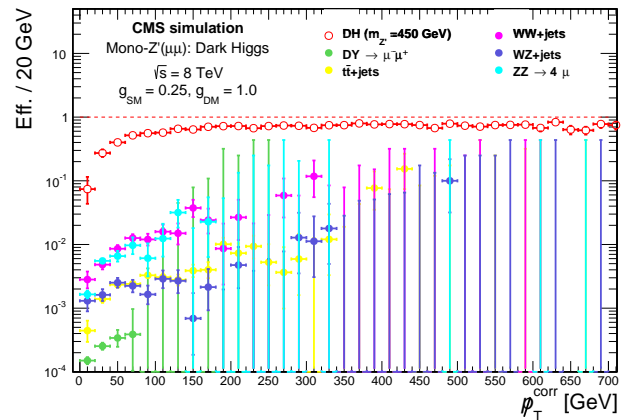


Figure 5 The efficiency presented as a function of \vec{p}_T^{corr} for the full selection of the analysis summarized in table VIII; for the SM backgrounds represented by solid dots with different corresponding colors and the DH model signal shown by hollow red dots.

VII. SYSTEMATIC UNCERTAINTIES

Several sources of experimental and theoretical systematic uncertainties are contributing to this analysis and affecting on the results. We start with the experimental systematic uncertainties; these uncertainty related to the luminosity of the CMS-2012 data is estimated to be 2.6% [47]. The uncertainty that arises from the determination of the muon detector acceptance and from the muon reconstruction efficiency ($A \times \epsilon$) has been found to be 3% [36]. The transverse muon momentum resolution uncertainty was 5%, while the misalignment in the detector geometry has an impact of 5% on the transverse momentum scale uncertainty per TeV [36]. Regarding the systematic uncertainties on the measurements of missing transverse momentum \vec{p}_T^{corr} , the uncertainty in the energy scale of low energy particles which is known as unclustered energy was found to be 10%, while 2-10% for jet energy scale and 6-15% for jet energy resolution [32]. Finally the theoretical sources of the systematics are related to the uncertainties in the parton distribution functions (PDF) choice. For the Drell-Yan cross section calculation, this uncertainty can be represented as a function of the invariant mass of the dimuon as $(2.67 + 3.03 \times 10^{-3} M_{\mu^+\mu^-} + 2.38 \times 10^{-6} M_{\mu^+\mu^-}^2)\%$ (in GeV) [36]. While PDF uncertainties for the WW and WZ processes were 5% and 6% respectively [13]. The summary of these sources of uncertainties and the corresponding values are indicated in table X.

	variable	requirements
	Trigger	HLT_Mu40_eta2p1
Preselection	High p_T muon ID	[43, 44]
	p_T^μ (GeV)	> 45
	η^μ (rad)	< 2.1
	$M_{\mu^+\mu^-}$ (GeV)	> 50
Tight selection	Mass window (GeV)	$(0.9 \times M_{Z'}) < M_{\mu^+\mu^-} < (M_{Z'} + 25)$
	$ p_T^{\mu^+\mu^-} - \cancel{p}_T^{\text{corr}} /p_T^{\mu^+\mu^-}$	< 0.6
	$\Delta\phi_{\mu^+\mu^-, \cancel{p}_T^{\text{corr}}}$ (rad)	> 2.6

Table VIII Summary of cut-based final events selection for the analysis.

Signal/Background	efficiency (%)
DH signal	67.0
$DY \rightarrow \mu^+\mu^-$	0.0196
$t\bar{t}$ + jets	0.24
WW + jets	0.84
WZ + jets	0.20
$ZZ \rightarrow 4\mu$	0.366

Table IX The over all efficiencies of the full selection, summarized in table VIII, for the dark Higgs scenario signal calculated at $M_{Z'} = 450$ GeV and the SM backgrounds.

Source	Uncertainty (%)
Luminosity (\mathcal{L})	2.6 [47]
$A \times \epsilon$	3 [36]
P_T resolution	5 [36]
P_T scale	5 [36]
Unclustered $\cancel{p}_T^{\text{corr}}$ scale	10 [32]
Jet energy scale	2-10 [32]
Jet energy resolution	6-15 [32]
PDF (Drell-Yan)	4.5 [36]
PDF (ZZ)	5 [13]
PDF (WZ)	6 [13]

Table X Different sources of systematic uncertainties estimated and the corresponding values.

VIII. RESULTS

For the dimuon channel, a shape-based analysis is employed. The missing transverse momentum distributions ($\cancel{p}_T^{\text{corr}}$) act as a good discriminant variable since the signal processes result in relatively larger $\cancel{p}_T^{\text{corr}}$ values than those of the SM backgrounds.

The missing transverse momentum distribution, after the final events selection, is shown in figure 6, which shows a significant decrease of SM background processes with the use of the analysis final selection summarized in table VIII. The number of dimuon events passing the final selection (summarized in VIII) for each of the SM background processes, the DH model (with $M_{Z'} = 450$ GeV) and the EFT model (with $\Lambda = 2$ TeV) corresponding to an integrated luminosity of 19.7 fb^{-1} are shown in table XI. Uncertainties include both statistical and systematic

components, summed in quadrature.

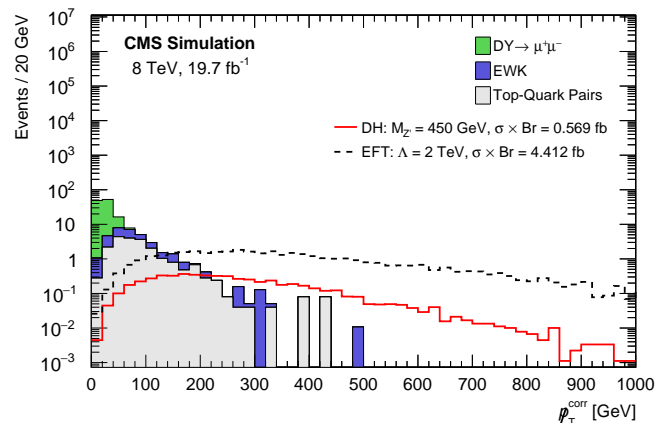


Figure 6 The distribution of the missing transverse momentum, after the final selection cuts listed in table VIII, for the SM background predictions, the signals of the model corresponding to the DH scenario with $M_{Z'} = 450$ GeV and the EFT scenario with cutoff scale $\Lambda = 2$ TeV are superimposed. The signals are normalized to the product of cross section times the $Z' \rightarrow \mu^+\mu^-$ branching ratio.

A. Statistical interpretation

In order to make a statistical interpretation of our results, we use the asymptotic approximation of the distribution of the profile likelihood-based statistical test described in details in [48]. This approach was used to investigate the possibility of the rejection of the null hypothesis (the SM background only hypothesis) in favor of the signal hypothesis (the dark Higgs scenario hypothesis) and used to construct the confidence intervals within 1 or 2 standard deviation corresponding to 68% or 95% Confidence Levels (CL). The likelihood function used to fit the data is defined as

$$\mathcal{L}(\mu, \theta) = \prod_{i=1}^M \frac{(\mu s_i + b_i)^{n_i} e^{-(\mu s_i + b_i)}}{n_i!} \prod_{j=1}^k \frac{u_j^{m_j} e^{-u_j}}{m_j!},$$

Process	No. of events
$DY \rightarrow \mu^+ \mu^-$	104.8 ± 27.1
$t\bar{t} + jets$	20.3 ± 6.6
$WW + jets$	12.7 ± 4.7
$WZ + jets$	1.2 ± 1.2
$ZZ \rightarrow 4\mu$	0.2 ± 0.5
Sum Bkgs	139.1 ± 35.3
Dark Higgs (at $M_{Z'} = 450$ GeV)	5.5 ± 2.7
EFT (at $M_{Z'} = 450$ GeV)	39.2 ± 11.3

Table XI The number of dimuon events passing the analysis final selection (summarized in table VIII) for each SM backgrounds, the DH model and the EFT model; corresponding to an integrated luminosity of 19.7 fb^{-1} . Uncertainties include both statistical and systematic components, summed in quadrature.

where μ is the signal strength, and defined as ratio between the signal yield and those of the prediction from simulation, which is the parameter of interest (POI) in this analysis, and θ represents the other nuisance parameters with an impact included in the equation on the second II-product. While s_i and b_i are number of signal and background events, respectively, as estimated from MC simulation per each bin. Finally u_j is a function of θ that gives the expectation value for each bin in the control sample used to constrain this nuisance parameters. It is a shape analysis based on the missing transverse momentum distributions.

B. Exclusion limits

We construct the confidence intervals for the signal strengths as a function of the mass of the new Z' boson ($M_{Z'}$) shown in figure 7, and with the mass of the stable dark sector particle M_χ shown in figure 8 for the DH simplified scenario, the confidence intervals for the signal strengths as a function of Λ for the EFT approach of the theory is presented in figure 9 as well. We exclude Z' production in the mass range between 470 - 550 GeV from the expected median as illustrated in figure 7. We also exclude DM particle (χ) production in the mass range between 170 - 200 GeV from expected median as shown in figure 8. For the EFT scenario, the range between 3670 - 3790 GeV is excluded for the model cutoff scale of the EFT(Λ), as shown in figure 9. These exclusion limits are estimated at 95% confidence level.

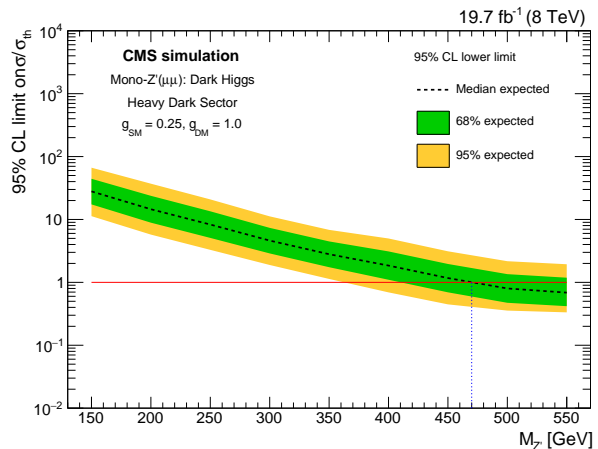


Figure 7 The limit at 95% CL on the expected $\sigma/\sigma_{\text{theory}}$ for the Dark Higgs scenario for the Z' dimuon decay of the Mono- Z' model. Distribution is shown as a function of $M_{Z'}$ for the heavy dark sector mass assumption shown in table I. The inner and outer shaded bands show the 68 and 95% CL uncertainties in the expected limits, respectively. The horizontal red line refers to $\sigma/\sigma_{\text{theory}} = 1$. The vertical blue dashed line point to the intersection of expectation with the case where $\sigma = \sigma_{\text{theory}}$.

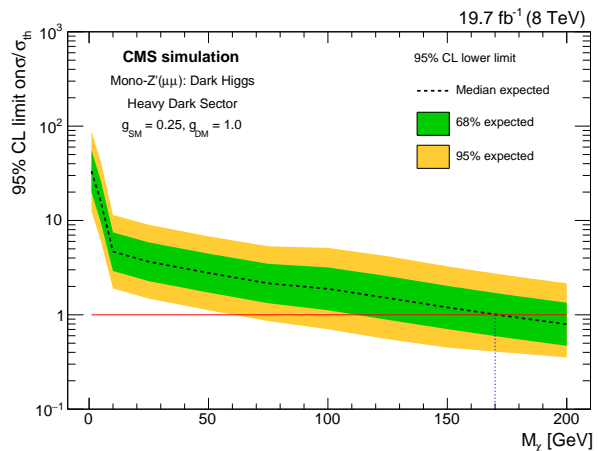


Figure 8 The limit at 95% CL on the expected $\sigma/\sigma_{\text{theory}}$ for the Dark Higgs scenario for the Z' dimuon decay of the Mono- Z' model. Distribution is shown as a function of M_χ for different values of the Z' mass. The inner and outer shaded bands show the 68 and 95% CL uncertainties in the expected limits, respectively. The horizontal red line refers to $\sigma/\sigma_{\text{theory}} = 1$. The vertical blue dashed line point to the intersection of expectation with the case where $\sigma = \sigma_{\text{theory}}$.

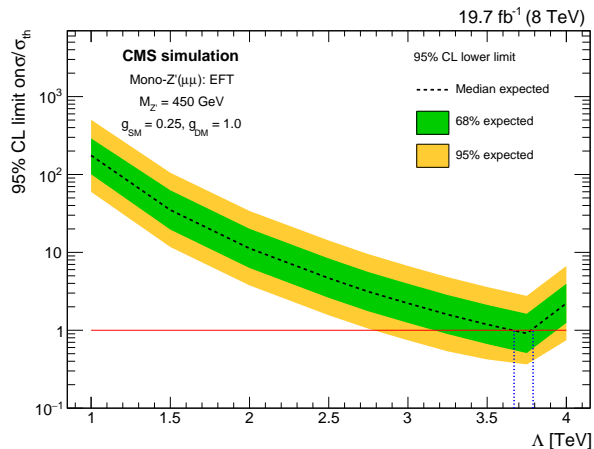


Figure 9 The limit at 95% CL on the expected $\sigma/\sigma_{\text{theory}}$ for the EFT scenario for the Z' dimuon decay of the Mono- Z' model. Distribution is shown as a function of the EFT cutoff scale (Λ). The inner and outer shaded bands show the 68 and 95% CL uncertainties in the expected limits, respectively. The horizontal red line refers to $\sigma/\sigma_{\text{theory}} = 1$. The vertical blue dashed lines point to the intersection of expectation with the case where $\sigma = \sigma_{\text{theory}}$.

IX. SUMMARY

A search for dark matter particles produced in association with a heavy gauge boson Z' has been performed. In this search we used MC samples which are taken from the open simulated files produced by the CMS collaboration for proton-proton collisions at $\sqrt{s} = 8$ TeV, the analysis was optimized for the full LHC run-I integrated luminosity (19.7 fb^{-1}). Results from muonic decay mode of Z' are presented, along with the statistical and system-

atic combination of uncertainties. One benchmark signal corresponding to the dark Higgs scenario was used with different choices of the mediator (Z') mass points. The 95% CL limits on the expected $\sigma/\sigma_{\text{theory}}$ of dark matter in a dark Higgs scenario extended by a Z' boson is set. These limits constitute the most stringent limits on the parameters ($M_{Z'}$ and M_χ) of this model. For the mass of Z' ($M_{Z'}$), the ranges between 470 - 550 GeV from expected median have been excluded, while excluding the ranges between 170 - 200 GeV from expected median for the mass of the dark matter χ (M_χ). In addition, the effective field theory (EFT) formalism of the mono- Z' model was used for interpreting the result. Limit was set on EFT cutoff scale (Λ), thus Λ range between 3.67 - 3.79 TeV is excluded.

We are planning to repeat the study with CMS full run-II data with larger centre-of-mass energy ($\sqrt{s} = 13$ TeV) and data integrated luminosity ($\mathcal{L} = 137 \text{ fb}^{-1}$).

ACKNOWLEDGMENTS

M. A. Louka wish to acknowledge the support of the Centre for Theoretical Physics (CTP) at the British University in Egypt (BUE) for the financial support to this work. The authors of this paper would like to thank Tongyan Lin, one of the authors of [17], for her useful discussions about the theoretical models, crosschecking of the results and for sharing with us the different scenarios Madgraph cards that were used for the events generation. We want to express our deepest thank to Nicola De Filipis from the politecnico di Bari/INFN for allowing us to use the computing facilities to produce and hosting our ntuples at Bari tier 2 servers. Finally we would like to thank Michele Gallinaro from LIP/Lisbon for his useful discussions about our results.

-
- [1] F. Zwicky, *The Redshift of the Extragalactic Nebulae*, Helv. Phys. Acta, Vol. 6, p. 110-127, 1933 [iNSPIRE-HEP].
 - [2] Yoshiaki SOFUE and Vera Rubin, *Rotation Curves of Spiral Galaxies*, Ann.Rev.Astron.Astrophys. 39 (2001) 137-174 [arXiv:astro-ph/0010594] [iNSPIRE-HEP].
 - [3] Scherrer, Robert J. and Turner, Michael S. *On the relic, cosmic abundance of stable, weakly interacting massive particles*, Phys. Rev. D 33 (1986) 1585 [iNSPIRE-HEP].
 - [4] Planck Collaboration, *Planck 2015 results. XIII. Cosmological parameters*, Astron. Astrophys. 594 (2016) A13 [arXiv:1502.01589] [iNSPIRE-HEP].
 - [5] Trimble, Virginia, *Existence and Nature of Dark Matter in the Universe*, Annual Review of Astronomy and Astrophysics, Vol.25 (1987) 425-472 [iNSPIRE-HEP].
 - [6] Bertone, Gianfranco and Hooper, Dan and Si, *Particle dark matter: Evidence, candidates and constraints*, Phys. Rept. 405 (2005) 279-390 [arXiv:hep-ph/0404175] [iNSPIRE-HEP].
 - [7] L. Bergstrom, *Non-baryonic dark matter: observational evidence and detection methods*, Rept. Prog. Phys. 63 (2000) 793 [arXiv:hep-ph/0002126] [iNSPIRE-HEP].
 - [8] K. Abazajian, G. M. Fuller and M. Patel, *Sterile neutrino hot, warm, and cold dark matter*, Phys. Rev. D 64 (2001) 023501 [arXiv:astro-ph/0101524] [iNSPIRE-HEP].
 - [9] Lage, C and Farrar, G, *The bullet cluster is not a cosmological anomaly*, JCAP, vol. 2015, no. 2, 038. <https://doi.org/10.1088/1475-7516/2015/02/038>.
 - [10] CMS Collaboration, *Search for new physics in final states with an energetic jet or a hadronically decaying W or Z boson and transverse momentum imbalance at $\sqrt{s} = 13$ TeV*, Phys. Rev. D 97 (2018) 092005. [arXiv:1712.02345] [hep-ex].
 - [11] CMS Collaboration, *Search for new physics in the monophoton final state in proton-proton collisions at $\sqrt{s} = 13$ TeV*, JHEP. 10 (2017) 073, [arXiv:1706.03794v2]

- [11] [hep-ex].
- [12] CMS Collaboration, *Search for dark matter particles produced in association with a Higgs boson in proton-proton collisions at $\sqrt{s} = 13$ TeV*, *JHEP* 03 (2020) 025, [arXiv:1908.01713v2] [hep-ex].
- [13] CMS Collaboration, *Search for dark matter and unparticles produced in association with a Z boson in proton-proton collisions at $\sqrt{s} = 8$ TeV*, *Phys. Rev. D* 93, 052011 (2016) [arXiv:1511.09375] [hep-ex].
- [14] CMS Collaboration, *Search for dark matter produced in association with a leptonically decaying Z boson in proton-proton collisions at $\sqrt{s} = 13$ TeV*, *Eur. Phys. J. C* 81 (2021) 13 [arXiv:2008.04735] [hep-ex].
- [15] Boveia, Antonio and Doglioni, Caterina, *Dark Matter Searches at Colliders*, *Ann. Rev. Nucl. Part. Sci.* 68 (2018) 429-459 [arXiv:1810.12238] [hep-ex].
- [16] Krovi Anirudh, Low Ian and Zhang Yue, dark matter searches at the LHC: mono-X versus darkonium channels. *JHEP* 10 (2018) 026 [arXiv:1807.07972] [hep-ph].
- [17] Marcelo Autran, Kevin Bauer, Tongyan Lin and Daniel Whiteson, *Mono-Z: searches for dark matter in events with a resonance and missing transverse energy*. *Physical Review D* 92 (2015) 035007 [arXiv:1504.01386] [hep-ph].
- [18] Paul Langacker, *The physics of heavy Z' gauge bosons*, *Rev. Mod. Phys.* 81 (2009) 1199-1228 [arXiv:0801.1345] [hep-ph].
- [19] Cheng-Wei Chiang, Takaaki Nomurad and Kei Yagyu, *Phenomenology of E 6-inspired leptophobic Z' boson at the LHC*, *JHEP* (2014) [arXiv:1402.5579] [hep-ph].
- [20] Digesh Raut, *gauged U(1) extension of the SM and Phenomenology*, PhD U. Alabama, Tuscaloosa (2018) [INSPIRE-HEP].
- [21] Robert Foot, X.G. He, H. Lew and R.R. Volkas, *Model for a light Z-prime boson*, *Phys.Rev.D* 50 (1994) 4571-4580 [arXiv:9401250] [hep-ph].
- [22] ATLAS Collaboration, *Search for dark matter in events with a hadronically decaying vector boson and missing transverse momentum in pp collisions at $\sqrt{s} = 13$ TeV with the ATLAS detector*, *JHEP* 10 (2018) 180 [arXiv:1807.11471] [hep-ex].
- [23] J. Alcaraz et al. (ALEPH Collaboration, DELPHI Collaboration, L3 Collaboration, OPAL Collaboration, LEP Electroweak Working Group) (2006), hep-ex/0612034.
- [24] The CMS Collaboration, *Software Framework for CMS Open Data Analysis*, <http://opendata.cern.ch/docs/about-cms>.
- [25] Aram Apyan, William Cuozzo, Markus Klute, Yoshihiro Saito, Matthias Schott and Bereket Sintayehu, *Opportunities and challenges of Standard Model production cross section measurements in proton-proton collisions at $\sqrt{s} = 8$ TeV using CMS Open Data*, *JINST* 15 (2020) [arXiv:1907.08197] [hep-ex].
- [26] J. Alwall, R. Frederix, S. Frixione, V. Hirschi, F. Maltoni, O. Mattelaer, H.-S. Shao, T. Stelzer, P. Torrielli & M. Zaro, *The automated computation of tree-level and next-to-leading order differential cross sections, and their matching to parton shower simulations*. *JHEP* 07 (2014) 079 [arXiv:1405.0301] [hep-ph].
- [27] CMS collaboration, *The CMS Experiment at the CERN LHC*, *JINST* 3 (2008) S08004 [INSPIRE-HEP].
- [28] CMS Physics, *Technical Design Report Volume I: Detector Performance and Software*, 2006.
- [29] M. Mulders, *Muon Reconstruction and Identification at CMS*, *Nuclear Physics B - Proceedings Supplements*, Volume 172, 2007, Pages 205-207, ISSN 0920-5632, <https://doi.org/10.1016/j.nuclphysbps.2007.08.049>.
- [30] CMS Collaboration, *Performance of CMS muon reconstruction in pp collision events at $\sqrt{s} = 7$ TeV*, *JINST* 7 (2012) [arXiv:1206.4071] [physics.ins-det].
- [31] CMS collaboration, *Particle-Flow Event Reconstruction in CMS and Performance for Jets, Taus, and MET*, Tech. Rep. CMS-PAS-PFT-09-001, CERN, Geneva, Apr, 2009.
- [32] CMS Collaboration, *Performance of the CMS missing transverse energy reconstruction in pp data at $\sqrt{s} = 8$ TeV*, *JINST* 10 (2015) P02006, [arXiv:1411.0511] [physics.ins-det].
- [33] Torbjorn sjostrand, stephen Mrenna and peter skands, *PYTHIA 6.4 Physics and Manual*, *JHEP* 05 (2006) 026 [arXiv:hep-ph/0603175].
- [34] E. Re, *Single-top Wt-channel production matched with parton showers using the POWHEG method*, *Eur. Phys. J. C* 71 (2011) 1547 [arXiv:1009.2450] [INSPIRE].
- [35] CMS Collaboration, Thomas McCauley, *Open Data at CMS: Status and Plans.*, PoS LHCP2019 (2019) 260 [INSPIRE-HEP].
- [36] CMS Collaboration, *Search for physics beyond the standard model in dilepton mass spectra in proton-proton collisions at $\sqrt{s} = 8$ TeV*, *JHEP* 04 (2015) 025 [arXiv:1412.6302] [hep-ex].
- [37] CMS Collaboration, *CMS list of validated runs for primary datasets of 2012 data taking*, CERN Open Data Portal. DOI:10.7483/OPENDATA.CMS.C00V.SE32,
- [38] CMS collaboration, *Simulated dataset DYToMuMu_M-20_CT10.8TeV-powheg-pythia6 in AODSIM format for 2012 collision data*. CERN Open Data Portal: <http://opendata.cern.ch/record/774>,
- [39] CMS collaboration, *Simulated dataset TTJets_FullLeptMGDecays_8TeV-madgraph in AODSIM format for 2012 collision data*. CERN Open Data Portal: <http://opendata.cern.ch/record/9577>.
- [40] CMS collaboration, *Simulated dataset WWJetsTo2L2Nu_TuneZ2star_8TeV-madgraph-tauola in AODSIM format for 2012 collision data*. CERN Open Data Portal: <http://opendata.cern.ch/record/9971>.
- [41] CMS collaboration, *Simulated dataset WZJetsTo3LNu_TuneZ2.8TeV-madgraph-tauola in AODSIM format for 2012 collision data*. CERN Open Data Portal: <http://opendata.cern.ch/record/9983>.
- [42] CMS collaboration, *Simulated dataset ZZTo4mu_8TeV-powheg-pythia6 in AODSIM format for 2012 collision data*. CERN Open Data Portal: <http://opendata.cern.ch/record/10071>.
- [43] CMS Collaboration, *Search for Resonances in the Dilepton Mass Distribution in pp Collisions at $\sqrt{s} = 7$ TeV*, *JHEP* 1105 093 (2011) [arXiv:1103.0981] [hep-ex].
- [44] <https://twiki.cern.ch/twiki/bin/view/CMSPublic/SWGuideMuonId#HighPT.Muon>.
- [45] Alexander Spiridonov, *An Approach To Global Vertex Fitting*, DESY-IfH Zeuthen / IHEP Protvino.
- [46] R. Frühwirth, *Application of Kalman filtering to track and vertex fitting*, *Nuclear Instruments and Methods in Physics Research Section A: Accelerators, Spectrometers, Detectors and Associated Equipment*, Volume 262, Issues 2-3, 1987, Pages 444-450, ISSN 0168-9002, [https://doi.org/10.1016/0168-9002\(87\)90887-4](https://doi.org/10.1016/0168-9002(87)90887-4).
- [47] CMS Collaboration, *CMS Luminosity Based on Pixel Cluster Counting - Summer 2013 Update*, CMS Physics Analysis Summary CMS-PAS-LUM-13-001 (2013).

[48] Glen Cowan , Kyle Cranmer , Eilam Gross , Ofer Vitells, *Asymptotic formulae for likelihood-based tests*

of new physics, Eur. Phys. J. C 71, 1554 (2011) [[arXiv:1007.1727](#)] [[physics.data-an](#)].